MULTI-TARGET TRACKING USING JOINT PROBABILISTIC DATA ASSOCIATION

Thomas E. Fortmann
Bolt Beranek & Newman Inc.
50 Moulton Street
Cambridge, MA 02238

Yaakov Bar-Shalom
Dept. of E.E. & C.S.
Univ. of Connecticut
Storrs, CT 06268

Molly Scheffé
Bolt Beranek & Newman Inc.
50 Moulton Street
Cambridge, MA 02238

Abstract

The Probabilistic Data Association (PDA) method, which is based on computing the posterior probability of each candidate measurement found in a validation gate, assumes that only one real target is present and all other measurements are Poisson-distributed clutter. In this paper, some new theoretical results are presented on the Joint Probabilistic Data Association (JPDA) algorithm, in which joint posterior probabilities are computed for multiple targets in Poisson clutter. The algorithm is applied to a passive sonar tracking problem with multiple sensors and targets, in which a target is not fully observable from a single sensor. Targets are modeled with four geographic states, two or more acoustic states, and realistic (i.e. low) probabilities of detection at each sample time. Simulation results are presented for two heavily interfering targets; these illustrate the dramatic improvements obtained by computing joint probabilities.

1. Introduction

The problems and issues involved in multi-target ocean tracking using a heterogeneous set of passive acoustic measurements were outlined in [F1]; chief among these are data association and maneuver detection. An approach to solving these problems was also described. The resulting experimental algorithm involves an extended Kalman filter (EKF) with both geographic and acoustic states, and handles measurement vectors such as bearing/frequency and delay/Doppler difference. Fundamental to the tracking algorithm is a *probabilistic data association* (PDA) scheme based on [B1], in which posterior probabilities are computed for all current candidate measurements in a validation gate and used to form a weighted sum of innovations for processing in the EKF. An appropriate correction term in the Riccati equation accounts for the uncertainty in measurement origin, and the resulting state estimate is the conditional expectation, subject to the assumption that the state estimate is Gaussian prior to each update. This questionable assumption leads to quite acceptable results in practice.

This research was supported by the Office of Naval Research under Contracts N00014-80-C-0270 and N00014-78-C-0259.

In addition to the basic PDA scheme, a multi-hypothesis structure is used for other decision making, including maneuver detection/correction, track initiation, and particularly difficult data association decisions. Only the PDA mechanisms will be considered here. The entire tracking system has been run successfully in real-time experiments.

The basic PDA algorithm assumes that each target is isolated from all other targets: false measurements in a validation gate are modeled as independent clutter points drawn from a Poisson distribution with density λ, and detection of a target is an independent event at each sample time with probability P_D.

In the ocean, the false measurements often originate from other targets and cannot truly be modeled as independent Poisson clutter points. Moreover, with passive measurements interference is probable at relatively low target densities; for example, geographically distant targets can lie at the same azimuth and be nearly indistinguishable from a single sensor. Nevertheless, our experience with real data indicates that many of these detections are so spurious that the interfering targets are effectively untrackable, and in practice the Poisson clutter assumption usually provides acceptable performance.

The Poisson assumption breaks down and performance degrades significantly when it is applied to an interfering target detected consistently by one or more sensors. In this case, the target is usually trackable and the PDA algorithm can be extended to correct for the discrete interference by computing the posterior probabilities *jointly* across clusters of targets; only the clutter is then modeled as Poisson. In the initial derivation [B3], some inappropriate assumptions led to erroneous prior probabilities, and the combinatorics of maintaining separate validation gates for each target made it very difficult to implement. In Section 2 of this paper we derive a simplified *joint probabilistic data association* (JPDA) algorithm for multiple targets in Poisson clutter. In Section 3 the performance improvements gained with the JPDA algorithm are illustrated using simulated data from two heavily interfering targets.

This is a *target-oriented* approach, in the sense that a set of established targets is used to form gates in measurement space and to compute posterior probabilities, in contrast to the *measurement-oriented* algorithm of [R1], where each measurement is considered in turn and hypothesized to have come from either some

0191-2216/80/0000-0807$00.75 © 1980 IEEE

established track or a new target. The difference between these two points of view is largely philosophical, since they lead to equivalent expressions for the posterior probabilities. Clutter densities are typically quite high in the ocean environment and neither position nor velocity is fully observable from a single passive measurement. These two characteristics make it essentially intractable to hypothesize a new track for each individual measurement, and in our approach targets are initiated by a separate operator-interactive process.

This is also a *non-backscan* (or zero-scan) approach, meaning that all hypotheses are combined after computation of the probabilities, for each target at each time step. While it can be extended to retain n scans as in [S1], this would lead to enormous memory requirements because of the relatively high clutter densities (0.2-2.0 false detections per gate) and the large number of separate measured variables (3-12 validation gates per target) that are typically encountered. Moreover, because of the spurious nature of many of the false detections, we strongly suspect that the JPDA is a more effective "memory" mechanism than a brute-force n-scan algorithm in this environment. Retaining multiple scans would also cause enormous complications for the maneuver detection and hypothesis-testing machinery that is built on top of the JPDA tracker.

2. Joint PDA Algorithm

The geographic/acoustic state equations and other details of the EKF tracker were described in [F1] and will not be repeated here. The data association is done by forming validation gates about the predicted measurements. In order to keep the notation tractable, consider a single measurement vector† (e.g. bearing/frequency from sensor A) and a single cluster†† of targets (established tracks) numbered t=1,...,T at a given time k. The set of m measurements associated with this cluster (i.e., found in the validation gates for targets 1,...,T) is denoted

$$Z(k) = \{\underline{y}_j\}_{j=1}^{m} \tag{1}$$

and the entire set of measurements up to time k is

$$Z^k = \{Z(k), Z^{k-1}\} \tag{2}$$

The argument k will be suppressed except in Z(k) and Z^k. Each measurement belongs either to one of the T targets or to the set of false measurements (clutter), which is denoted by target number t=0.

Denoting the predicted measurement for target t by $\hat{\underline{y}}^t$, the innovation corresponding to measurement j is

$$\tilde{\underline{y}}_j^t \triangleq \underline{y}_j - \hat{\underline{y}}^t \tag{3}$$

†This is $\underline{y}_i$ in the notation of [F1], but the i will be suppressed here.

††A cluster is a set of targets whose validation gates are "connected" by measurements lying in their intersections [B3,R1]. Note that a different measurement vector (e.g. time/Doppler difference as measured between sensors B and C) will lead to different target clusters.

The state estimate for target t is updated in the EKF using the weighted (or combined) innovation

$$\tilde{\underline{y}}^t = \sum_{j=1}^{m} \beta_j^t \tilde{\underline{y}}_j^t \tag{4}$$

where β_j^t is the posterior probability that measurement j originated from target t and β_0^t is the probability that none of the measurements originated from target t (i.e., it was not detected). The covariance equation is also corrected to account for the effects of association uncertainty [F1,B1,B2].

The PDA algorithm computes β_j^t, j=0,1,...,m, separately for each t, under the assumption that *all* measurements not associated with target t are false (i.e., Poisson-distributed clutter); the resulting expressions are given in [F1,B1,B2]. The JPDA algorithm described here computes β_j^t *jointly* across the set of T targets and clutter. From the point of view of any given target, this accounts for false measurements from both discrete interfering sources (other targets) and random clutter.

The key to the JPDA algorithm is evaluation of the conditional probabilities of the following joint events,

$$\underline{\chi} = \bigcap_{j=1}^{m} \chi_{jt_j} \tag{5}$$

where χ_{jt_j} is the event that measurement j originated from target t_j and $0 \le t_j \le T$. The *feasible events* are those for which no more than one measurement originates from each target, i.e.

$$j \neq \ell \text{ and } t_j > 0 \text{ implies } t_j \neq t_\ell \tag{6}$$

It is also convenient to define the binary variables

$$\tau_j(\underline{\chi}) \triangleq \begin{cases} 1 & \text{if } t_j > 0 \\ 0 & \text{if } t_j = 0 \end{cases} \tag{7}$$

which indicates whether measurement j is associated with any established target in event $\underline{\chi}$, and

$$\delta_t(\underline{\chi}) = \begin{cases} 1 & \text{if } t_j = t \text{ for some } j \\ 0 & \text{if } t_j \neq t \text{ for all } j \end{cases} \tag{8}$$

which indicates whether any measurement is associated with target t in event $\underline{\chi}$ (i.e. whether target t is detected).

For the purpose of deriving the joint probabilities, *no individual validation gates will be assumed for the various targets.* Instead, each measurement will be assumed validated for each target, i.e., every validation gate coincides with the entire surveillance region. This approach is adopted because the resulting equations are equivalent but simpler than if different validation gates are assumed for each target. The extra computational burden resulting from the consideration of events with negligible probability can be avoided with suitable logic limiting the probability calculations to events involving validated measurements. This logic, which has a negligible effect on the numerical results, is presented next, followed by a derivation of the joint event probabilities.

Validation Logic

The following validation matrix is defined,

$$\underline{\Omega} = [\omega_{jt}] \quad j=1,\ldots,m; \quad t=0,1,\ldots,T \qquad (9)$$

with binary elements to indicate if measurement j lies in the validation gate for target t. Index t=0 stands for "no target" and the corresponding column of $\underline{\Omega}$ has all units — each measurement could have originated from clutter or false alarm. A typical set of gates and the corresponding validation matrix is shown in Figure 1.

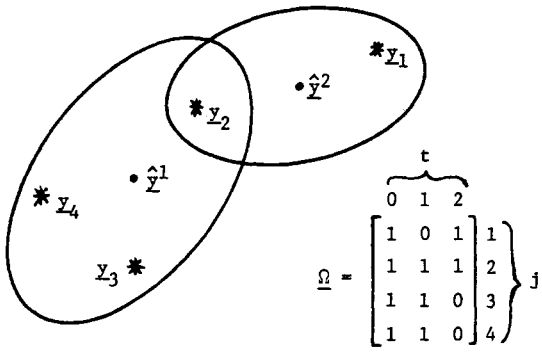

Figure 1. Typical gates and validation matrix

Each event $\underline{\chi}$ may be represented by a matrix

$$\hat{\underline{\Omega}}(\underline{\chi}) = [\hat{\omega}_{jt}(\underline{\chi})] \qquad (10)$$

consisting of the units in $\underline{\Omega}$ corresponding to the associations assumed in event $\underline{\chi}$. Thus

$$\hat{\omega}_{jt}(\underline{\chi}) = \begin{cases} 1 & \text{if } \chi_{jt} \text{ occurs} \\ 0 & \text{otherwise} \end{cases} \qquad (11)$$

Given considerable patience, one can construct an algorithm that scans $\underline{\Omega}$ and enumerates the matrices $\hat{\underline{\Omega}}(\underline{\chi})$ corresponding to the feasible events using the following rules:

1. Scan $\underline{\Omega}$ by rows and pick one unit per row for $\hat{\underline{\Omega}}$ (i.e., there can be only one origin for a measurement)
2. Only one unit from each column $t \geq 1$ can be taken (i.e., at most one measurement could have originated from a target). The number of units from column t=0 is not restricted.

In terms of the matrix $\hat{\underline{\Omega}}(\underline{\chi})$, the measurement association indicator (7) becomes

$$\tau_j(\underline{\chi}) = \sum_{t=1}^{T} \hat{\omega}_{jt}(\underline{\chi}) \qquad (12)$$

and the target indicator (8) is

$$\delta_t(\underline{\chi}) = \sum_{j=1}^{m} \hat{\omega}_{jt}(\underline{\chi}) \qquad (13)$$

Joint Probabilities

Using Bayes' rule, the probability of a joint event conditioned on all the measurements up to the present time is

$$P\{\underline{\chi}|Z^k\} = \frac{1}{c}\, p[Z(k)|\underline{\chi}, Z^{k-1}] P\{\underline{\chi}|Z^{k-1}\} \qquad (14)$$

where c is the normalization constant obtained by summing the r.h.s. over all $\underline{\chi}$.

The first term on the r.h.s. of (14) is

$$p[Z(k)|\underline{\chi}, Z^{k-1}] = \prod_{j=1}^{m} p[\underline{y}_j | \chi_{jt_j}, Z^{k-1}] \qquad (15)$$

The conditional probability density of an individual measurement is, using (7),

$$p[\underline{y}_j | \chi_{jt_j}, Z^{k-1}] = \begin{cases} f_{t_j}[\underline{y}_j] & \text{if } \tau_j(\underline{\chi})=1 \\ V^{-1} & \text{if } \tau_j(\underline{\chi})=0 \end{cases} \qquad (16)$$

where $f_{t_j}[\cdot]$ is the probability density of the predicted measurement from target t_j for time k and V is the volume of the entire surveillance region. The measurements not having originated from targets are assumed independently distributed with a uniform density in the entire surveillance region. The densities f_t are usually approximated as normal.

The second term on the r.h.s. of (14) is the prior (to time k) probability of a joint event. To obtain it, note that the total number of false measurements in event $\underline{\chi}$ is

$$\phi(\underline{\chi}) = \sum_{j=1}^{m} [1-\tau_j(\underline{\chi})] \qquad (17)$$

Then the number of events $\underline{\chi}$ in which the same set of targets is detected is given by the number of permutations of m (number of measurements) taken as $m-\phi(\underline{\chi})$ (number of detections):

$$P^m_{m-\phi(\underline{\chi})} = \frac{m!}{\phi(\underline{\chi})!} \qquad (18)$$

With this, the prior probability of event $\underline{\chi}$ is given by

$$P\{\underline{\chi}|Z^{k-1}\} = \frac{1}{m!/\phi!} \prod_{t:\delta_t=1} P_D^t \prod_{t:\delta_t=0} (1-P_D^t)\, \frac{e^{-\lambda V}(\lambda V)^{\phi}}{\phi!} \qquad (19)$$

where P_D^t is the probability of detection of target t, the number ϕ of false measurements is assumed Poisson distributed with parameter λV, λ is the density of false measurements, and the dependence of ϕ and δ_t on $\underline{\chi}$ has been dropped from the notation.

Combining (15), (16), and (19) into (14) yields

$$P\{\underline{\chi}|Z^k\} = \frac{V^{-\phi}}{c} \prod_{j:\tau_j=1} f_{t_j}[\underline{y}_j]\, \frac{\phi!}{m!} \cdot \prod_{t:\delta_t=1} P_D^t \prod_{t:\delta_t=0} (1-P_D^t)\, \frac{e^{-\lambda V}(\lambda V)^{\phi}}{\phi!} \qquad (20)$$

Note that m! and $e^{-\lambda V}$ appear in all the expressions. After several cancellations the final expression is obtained as

$$P\{\underline{\chi}|Z^k\} = \frac{\lambda^\phi}{c} \prod_{j:\tau_j=1} f_{t_j}[\underline{y}_j] \prod_{t:\delta_t=1} P_D^t \prod_{t:\delta_t=0} (1-P_D^t) \tag{21}$$

where c is the (new) normalization constant.

The probability β_j^t that measurement j belongs to target t may now be obtained by summing over all feasible events $\underline{\chi}$ for which this condition is true:

$$\beta_j^t = \sum_{\underline{\chi}} P\{\underline{\chi}|Z^k\}\hat{\omega}_{jt}(\underline{\chi}) \quad j=1,.,m; \quad t=0,1,.,T \tag{22}$$

$$\beta_0^t = 1 - \sum_{j=1}^{m} \beta_j^t \qquad t=0,1,.,T \tag{23}$$

These probabilities are used to form the combined innovation (4) for each target.

When $f_{t_j}[\cdot]$ is replaced by a Gaussian density, (21) becomes

$$P\{\underline{\chi}|Z^k\} = \frac{\lambda^\phi}{c} \prod_{j:\tau_j=1} \frac{\exp[-\frac{1}{2}(\tilde{y}_j^{t_j})'\underline{S}_{t_j}(\tilde{y}_j^{t_j})]}{(2\pi)^{\ell/2}|\underline{S}_{t_j}|^{1/2}} \cdot \prod_{t:\delta_t=1} P_D^t \prod_{t:\delta_t=0} (1-P_D^t) \tag{24}$$

where $\tilde{y}_j^{t_j}$ is the innovation defined in (3), $\underline{S}_{t_j}$ is the innovation covariance matrix from the t_j-th target, and ℓ is the dimension of $\underline{y}$.

Numerical overflows and underflows are common in the factor λ^ϕ and the normalization constant c, because the magnitude of λ (in units of 1/volume in the measurement space) is quite variable and ϕ can be 10 or more. The problem can be avoided simply by letting $1/\lambda$ be the unit of volume in evaluating (24), so that λ^ϕ is replaced by 1^ϕ. This change cancels out in the exponential factor, and it causes $|\underline{S}_{t_j}|^{1/2}$ to be multiplied by λ, yielding

$$P\{\underline{\chi}|Z^k\} = \frac{1}{c} \prod_{j:\tau_j=1} \frac{\exp[-\frac{1}{2}(\tilde{y}_j^{t_j})'\underline{S}_{t_j}(\tilde{y}_j^{t_j})]}{(2\pi)^{\ell/2}|\underline{S}_{t_j}|^{1/2}} \cdot \prod_{t:\delta_t=1} P_D^t \prod_{t:\delta_t=0} (1-P_D^t) \tag{25}$$

3. Tracking Results

A simulation program was used to create realistic passive sonar data on which the JPDA algorithm could be tested. One such data set contains measurement files of bearing/frequency lines and time/Doppler differences for two hypothetical targets, with a common 12 Hz source frequency and courses that result in severe interference. The target-sensor geometry is indicated in Figure 2. Targets 1 and 2 travel at 6 knots on courses of 100° and 80°, respectively, and cross midway through the 6-hour period shown.

Measurement data were created by dead reckoning target motion (no process noise), adding noise to the computed true measurements, and then adding clutter measurements (false detections). The standard deviation of the measurement noise was 5° for bearings, 80 mHz for frequency, 3.6 sec. for time difference, and 4 mHz for Doppler difference. The true measurement was detected at any given time with probability P_D=0.7. The number of clutter points was Poisson-distributed and their locations in the measurement space were uniformly distributed over a very broad region about the actual track. The clutter density was λ=0.25/Hz-deg for bearing/frequency and λ=.25/Hz-sec for time/Doppler difference; with varying gate sizes, this ranged from 0.2 to 2.0 false detections per gate.

Several tracks were made using this data; the initial 2-sigma confidence ellipse areas were about 100 mi^2, with course and speed confidences of ±20° and ±3 knots, respectively. In practice, one would use somewhat looser limits to initialize uncertain targets, but the object here was to simulate a situation in which the tracks are already several hours old before they intersect.

When the ordinary PDA filter (without multi-target logic) is confronted with this situation, the result is disastrous. As shown in Figure 3, both tracks lock onto a sort of "compromise" and end up lost midway between the two actual targets. This behavior is to be expected, since a basic assumption in the standard PDA algorithm (applied to each target in turn) is that measurements not originating from the target under consideration are random clutter points with a Poisson/uniform distribution.

The joint PDA method, described above in Section 2, corrects this situation by allowing the probabilistic weights used in data association to be computed jointly across all known targets. As shown in Figure 4, this improves the tracks dramatically, and the 2-sigma confidence ellipses contain the true position in all cases. Note that the ellipses are larger than those of Figure 3, particularly near the point of intersection, reflecting the fact that the algorithm "hedges" its decisions and relies more on dead reckoning when the targets are too close to determine with high confidence which measurement belongs to which target.

The JPDA-computed association probabilities of a measurement belonging to the correct target vs. the other one typically have ratios of .8/.2 or greater. As the targets draw nearer each other, the ratios switch rather abruptly to around .5/.5 (and the confidence ellipse areas increase accordingly); then they switch back again when the targets separate.

Table 1 illustrates the increased number of "correct" measurement decisions when the multi-target logic is employed. The numbers in the first column indicate how often the measurement from the correct target received a higher probability than any other measurement in the gate. The second column indicates how many times the other (interfering) target received the highest probability, and the third column does the same for clutter measurements. The difference is not as marked as Figures 3 and 4 might suggest. Nevertheless, as expected, the improvement is greatest in time/Doppler difference, corresponding to the most precise measurements of both position and velocity.

	Correct Target	Other Target	Clutter	Multi-target Logic
Brng/freq	49%	41%	10%	ON
Time/Doppler	66%	26%	8%	
Total	55%	36%	9%	
Brng/freq	45%	46%	9%	OFF
Time/Doppler	48%	46%	6%	
Total	46%	46%	8%	

Table 1: Percentage of decisions where highest probability was assigned to measurement from correct target, other target, or clutter.

Finally, tracks made using perfect data association are shown in Figure 5. Comparing these with Figure 4, it is clear that the JPDA tracker performs remarkably well despite the severe interference between targets. Indeed, by the end of the 6-hour period, the two sets of tracks are nearly identical.

As important as tracking accuracy is the tracker's own assessment of that accuracy, expressed by the covariance matrix. To compare this for the tracks of Figures 3-5, the filter consistency measure

$$r^2(k) = [\hat{\underline{x}}(k)-\underline{x}(k)]'\underline{P}^{-1}(k)[\hat{\underline{x}}(k)-\underline{x}(k)] \qquad (26)$$

was computed at each time k, where $\underline{x}(k)$ is the true state, $\hat{\underline{x}}(k)$ is the estimate, and $\underline{P}(k)$ is the covariance matrix computed on-line by the tracker. Mean-square and root-mean-square (RMS) values of this statistic over the 6-hour period (71 time steps) are given in Table 2, together with their theoretical values (r^2 is a chi-square random variable with 6 degrees of freedom).

Table 2 indicates that the ordinary PDA tracker is overoptimistic, having actual errors much larger than its calculated covariance would indicate. The JPDA tracker is about as consistent as the perfect data association tracker, and both are slightly pessimistic in comparison to the theoretical chi-square value.

Also shown in Table 2 are the final position errors (in nautical miles) for the same period. Fortuitously, the position error for Target 2 using the ordinary PDA is slightly better than the others. Nevertheless, the confusion of the ordinary PDA is evident from Figure 3.

4. Conclusion

Report-to-track correlation has been identified as one of the major problems in ocean surveillance [W1], and the results of this paper demonstrate the importance of correlating each report with all tracks simultaneously, rather than separately. The joint probabilistic data association framework is particularly well-suited to this task in the passive sonar environment, where additional measurements arise from both interfering targets and random clutter, detection probability is significantly less than 1, the measurement space is large and heterogeneous, a target's state is not fully observable from any single measurement, and maneuvers are common.

Continuing research in this and related areas includes assessment of tracking performance as a function of detection probability and clutter density (this has important implications for the setting of gains and thresholds in the signal processing algorithms that provide measurements to the tracker), extension of the likelihood function and other hypothesis-testing machinery to the JPDA situation, and the use of more complex models for the detection and clutter processes.

		Ordinary PDA	Joint PDA	Perfect DA	Theoretical Value
Target 1	$\overline{r^2}$	22.1	4.6	5.6	6
	$\sqrt{\overline{r^2}}$	4.7	2.2	2.4	2.4
	position error	5.4	6.6	5.6	-
Target 2	$\overline{r^2}$	10.8	2.7	3.8	6
	$\sqrt{\overline{r^2}}$	3.3	1.6	2.0	2.4
	position error	5.3	1.1	1.8	-

Table 2: Error statistics

References

[B1] Y. Bar-Shalom and E. Tse, "Tracking in a Cluttered Environment with Probabilistic Data Association," Automatica, Vol. 11, pp. 451-460, Sept. 1975. (Also in 1973 Symp. on Nonlinear Estimation.)

[B2] Y. Bar-Shalom, "Tracking Methods in a Multitarget Environment," IEEE Trans. Auto. Control, Vol. AC-23, pp. 618-626, Aug. 1978.

[B3] Y. Bar-Shalom, "Extension of the Probabilistic Data Association Filter to Multitarget Environment," Proc. Fifth Symp. on Nonlinear Estimation, San Diego, CA, Sept. 1974.

[F1] T. E. Fortmann and S. Baron, "Problems in Multitarget Sonar Tracking," Proc. 1978 IEEE Conf. on Decision and Control, San Diego, CA, Jan. 1979.

[R1] D. B. Reid, "An Algorithm for Tracking Multiple Targets," IEEE Trans. Auto. Control, Vol. AC-24, pp. 843-854, Dec. 1979.

[S1] R. Singer, R. Sea, and K. Housewright, "Derivation and Evaluation of Improved Tracking Filters for Use in Dense Multitarget Environments," IEEE Trans. Info. Theory, Vol. IT-20, pp. 423-432, July 1974. (Also in 1973 Symp. on Info. Theory.)

[W1] H. L. Weiner, W. W. Willman, I. R. Goodman, and J. H. Kullback, "Naval Ocean-Surveillance Correlation Handbook, 1978," NRL Report 8340, October 1979.

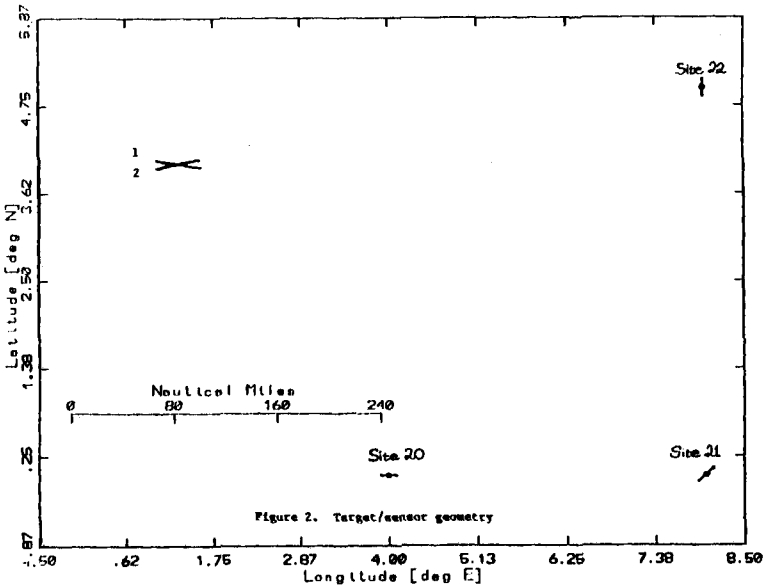

Figure 2. Target/sensor geometry

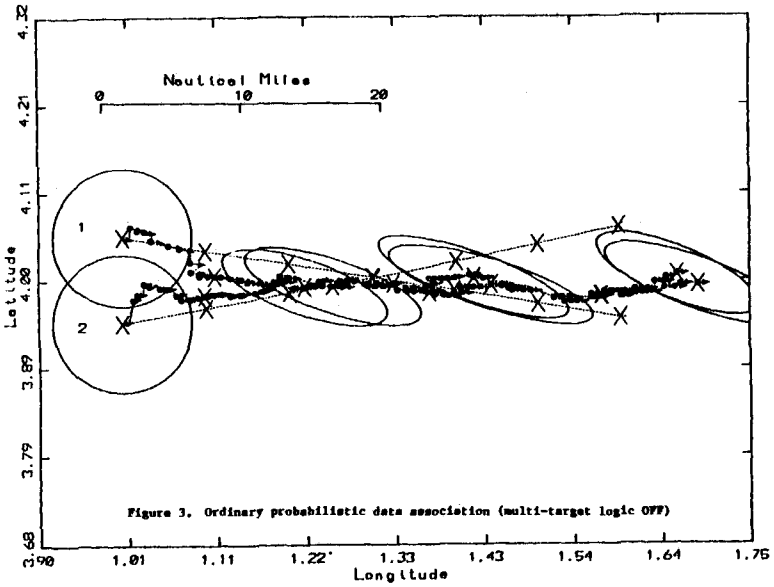

Figure 3. Ordinary probabilistic data association (multi-target logic OFF)

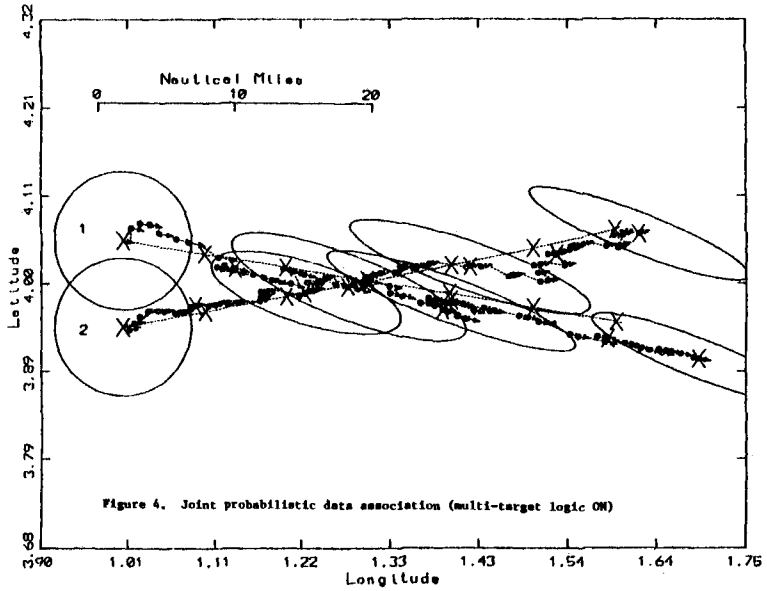

Figure 4. Joint probabilistic data association (multi-target logic ON)

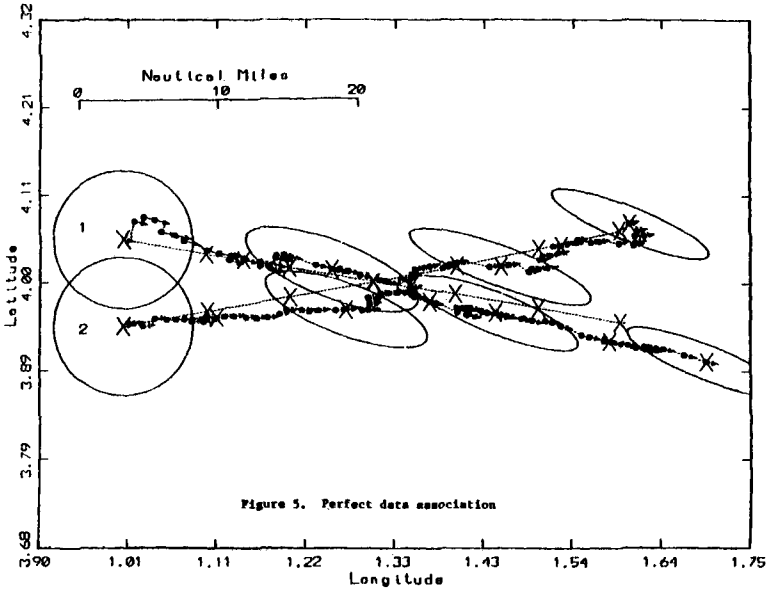

Figure 5. Perfect data association